Fifth Semi-Annual Progress Report

on

INVESTIGATION OF TECHNICAL PROBLEMS RELATED TO DEPLOYMENT AND RETRIEVAL OF SPINNING SATELLITES

NASA Grant NGR 39-009-162

Principal Investigator

Marshall H. Kaplan

Associate Professor of Aerospace Engineering

The Pennsylvania State University

University Park, Penna. 16802

Submitted to:

National Aeronautics and Space Administration

Washington, D.C. 20546

July 1972

TABLE OF CONTENTS

APPENDICES

I. INTRODUCTION

The subject grant (NGR 39-009-162) on technical problems related to deployment and retrieval of spinning satellites is at mid-term in a one-year extension of the original two-year grant. This is the fifth semi-annual status report on the project. During the past six months (1 January 1972 to 30 June 1972) work has progressed in the two major areas outlined in the new statement of work, Appendix A of the fourth progress report, January 1972. Quantitative analyses have been developed to the point where numerical results can be easily obtained in the optimal transfer trajectory problem. This effort should be completed within the next few months. Analyses of deployment dynamics and control of the paired-satellite concept (AMAPS) are progressing well and results are expected by the end of this year. A summary of accomplishments is offered in section III. Individual personnel assignments are cited in section II, and expected progress for the next grant period is summarized in section IV. Detailed descriptions of accomplishments are left for appendices.

Interaction with NASA and industry is considered essential to avoid duplication of effort and to provide helpful guidance. Recently (June 1) the principal investigator visited the Astronics Lab. at NASA-MSFC to discuss satellite retrieval problems. Just prior to that Mr. Heinz Fornoff presented a seminar at Penn State on the subject of manipulators in space. Such interactions have been very helpful in directing research tasks.

Dissemination of results is a primary function of such research grants. In connection with this grant a paper entitled "The Problem of Docking with a Passive Orbiting Object Which Possesses Angular Momentum," (See Appendix B, Fourth Progress Report, January 1972) will appear this Summer in Astronautical Research 1971, Proceedings of the 22nd I.A.F. Congress, published 1972. In addition, the paper entitled, "Attitude Dynamics and Control of an Apogee Motor Assembly with Paired Satellites," (See Appendix C, Fourth Progress Report, January 1972) has been published in the Journal of Spacecraft and Rockets, June 1972, page 410.

Notification has just recently been received that an abstract entitled, "The Problem of Deploying and Retrieving Spinning Payloads in Orbit," has been accepted to the Fifth Symposium on Automatic Control in Space, sponsored by the International Federation of Automatic Control (IFAC), to be held June 5-9, 1973 in Genoa, Italy. This abstract is included here as Appendix A.

II. PERSONNEL

The grant budget currently supports three graduate assistants on half-time schedules. This project is currently fully staffed with three master of science candidates (E. C. Thoms, R. J. Cenker, and A. A. Nadkarni). Two of these students (Thoms and Cenker) should be completing their theses during the latter part of 1972. These will be published as Astronautics Research Reports of the Aerospace Engineering Department of Penn State, and submitted to appropriate journals for wider dissemination.

Basic task assignments presented previously have not changed significantly. However, as progress is made interactions and objectives must be modified to reflect current and expected situations. Therefore, new project flow charts have been constructed showing current areas of study. These are presented in Figure 1.

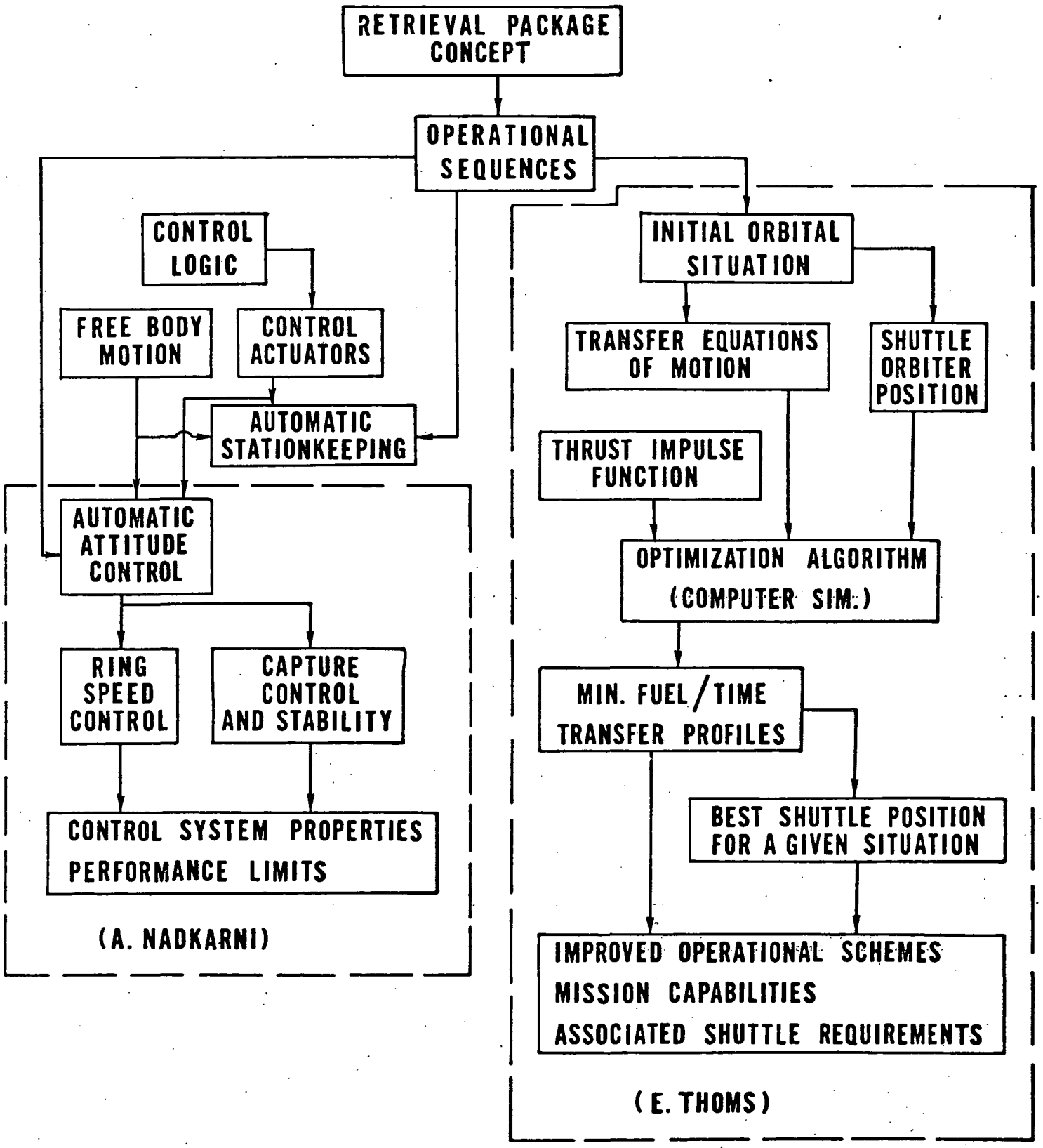

Figure 1. Project Flow Chart

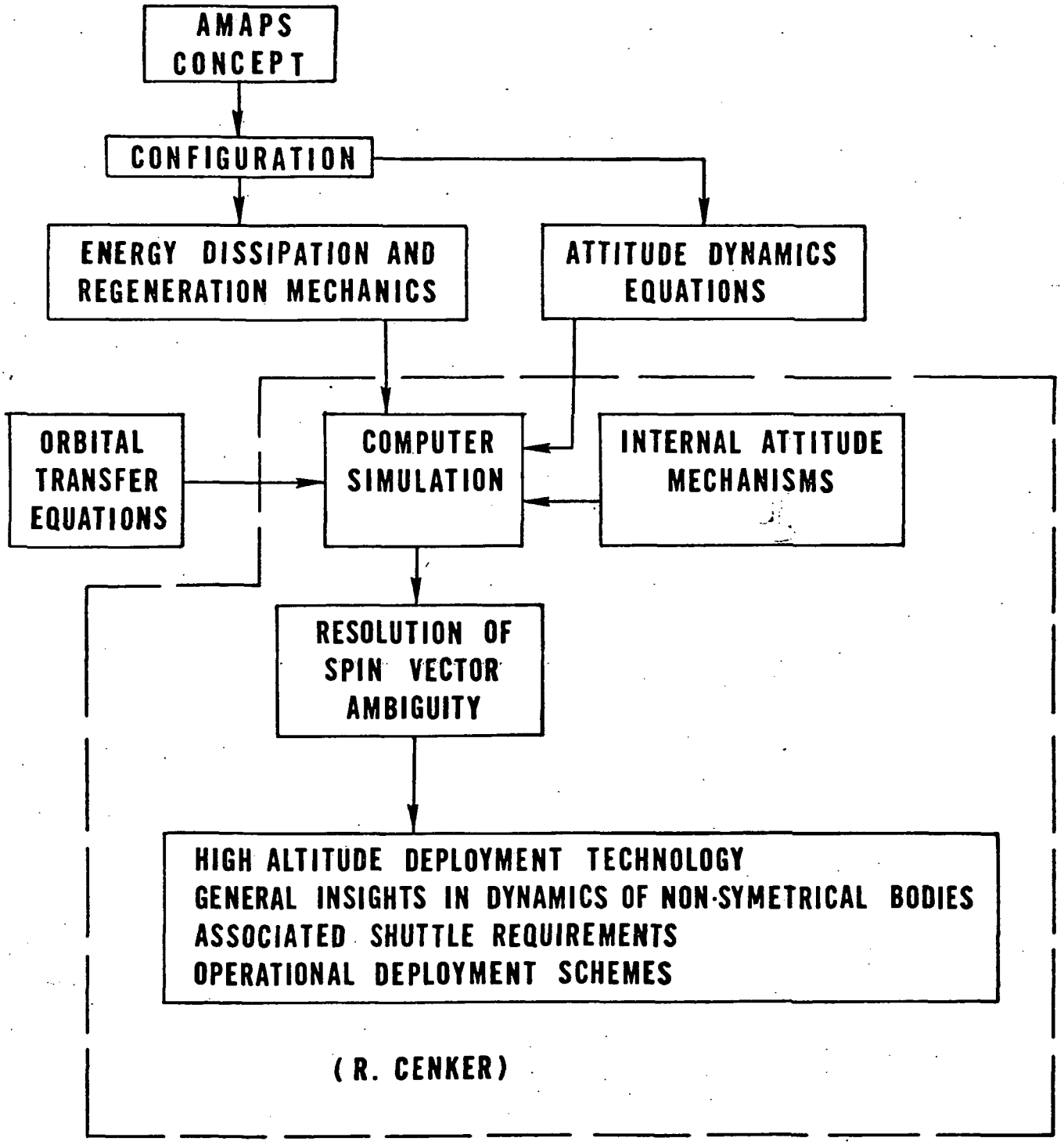

Figure 1. (continued)

III. PROGRESS TO DATE

The current one-year renewal of this project has permitted a significant increase in forthcoming results related to retrieval and deployment technology. Specific areas of concentration include optimal transfer trajectories for retrieval, attitude reorientation during deployment sequences, and automatic controls for retrieval spacecraft.

Retrieval package transfer trajectories between the orbiter and target can be optimized for minimum fuel or time through the use of optimal control techniques established in the literature. The problem considered here is nonlinear with two-point boundary values and is constrained at the terminal point because of the desired spin-axis alignment. Such problems require the use of a computer for solution. A detailed discussion of progress on this problem is presented as Appendix B.

The initial work reported in the Journal of Spacecraft article, "Attitude Dynamics and Control of an Apogee Motor Assembly with Paired Satellites," is continuing with the objective of active spin reorientation. Progress to date is concerned with developing relationships for tumbling dynamics of non-symmetrical satellites to determine limits on nutation angles, ratios of moments of inertia, and energy state. Such relationships define the critical point in energy level during passive spin axis transfer of an AMAPS type device at which final spin axis direction may be controlled most easily. A detailed discussion of this problem is presented in Appendix C.

As the retrieval package operational plan developed several controls problems arose in connection with attitude maintenance during the capture sequence. Such problems are especially important to more automated

missions for retrieval, e.g., during synchronous orbit missions. Therefore, work has continued on synthesizing control laws for the various situations of interest. Specifically, considerations include the case of general target spin vector misalignment relative to the despin ring and control of the ring speed during capture. Control system developments for these functions are discussed in Appendix D.

IV. FUTURE TASKS

Efforts will continue in the areas of optimal transfer trajectories, spin reorientation control, and control system synthesis for retrieval package functions. Optimal three-dimensional transfer trajectories will be generated for various parking positions of the orbiter and target spin orientations. Comparisons will be made with results from the conjugate-gradient technique and other methods. Recommendations concerning the best stand-off position for the orbiter will also be included. This task should be complete by the end of 1972.

The work on spin reorientation will continue through computer simulations of various control schemes to insure proper final spin vector direction. Methods in which moments of inertia are varied and energy is changed will be considered. Appropriate mechanisms will be conceived for such applications. This task should also be completed by the end of 1972.

Activities related to automatic operations will continue and, hopefully, develop into a phase of a new grant involving studies of self-contained high-altitude deployment packages, multiple and automated retrieval missions, and high-altitude retrieval techniques. A great deal of knowledge relevant to orbital retrieval and payload deployment has been gained, and each new area of technology has led to further questions about retrieval and deployment.

APPENDIX A

Abstract for Fifth Symposium on Automatic Control in Space
(Genoa, Italy, June 5-9, 1973. Sponsored by IFAC)

The Problem of Deploying and Retrieving Spinning Payloads in Orbit*

Marshall H. Kaplan
Associate Professor of Aerospace Engineering
The Pennsylvania State University
University Park, Pa. 16802
U.S.A.

ABSTRACT

Two of the primary missions for the space shuttle system will be the deployment and retrieval of payloads. Many of these will be spinning for stability. A large number of old satellites and other debris in orbit are spinning due to initial deployment maneuvers or later mishaps. In either case, the presence of passive angular momentum requires special techniques which will not endanger the shuttle orbiter vehicle. Separate spacecraft, operated from the shuttle, may be used to deploy and retrieve spinning objects. A conceptual design of such vehicles has been proposed and many of the technical problems have been defined.[1]

The paper proposed here will consider many of the "key" problem areas related to dynamics and control of deployment and retrieval in both low and high orbits. Topics will include: (1) optimal transfer of a retrieval package from shuttle to spinning objects such that approach is accomplished along the spin axis, (2) control of spin reorientation during high altitude deployment, and (3) automatic stationkeeping of the shuttle

---

*This work is supported by NASA Grant NGR 39-009-162.

relative to a retrieval target. The second item represents an extension of work on a special technique for deploying pairs of high altitude satellites without the use of an orbit-to-orbit tug.[2] During large angle reorientation of a passive semi-rigid body, there arises an ambiguity in final pointing direction of the stable spin axis. The elimination of this ambiguity can be accomplished by an active mechanism within the body. This will be discussed in detail and quantitative results presented.

The optimal transfer problem arises in order to minimize fuel or time during the retrieval of a spinning object. In the case of a multiple retrieval mission the intermediate spacecraft would have limited fuel for maneuvers. In other situations time could be the critical factor. The requirement that final approach of the retrieval vehicle be along the object spin axis represents an end constraint which significantly complicated the problem. Automatic stationkeeping of the shuttle during these maneuvers is closely related to the transfer trajectories since this represents an optimum stand-off position for the orbiter. Considerations for selecting a combination of parking positions and transfer trajectories will be included.

References

1. Kaplan, M. H. et al., "Dynamics and Control for Orbital Retrieval Operations Using the Space Shuttle," NASA-KSC TR-1113, Vol. 1, May 1971, pp. 175-201.

2. Kaplan, M. H. and Beck, N. M., "Attitude Dynamics and Control of an Apogee Motor Assembly with Paired Satellites," Journal of Spacecraft and Rockets, June 1972, pp. 410-415.

APPENDIX B

Optimal Retrieval Transfer Trajectories

(E. C. Thoms)

I. Introduction

During a retrieval mission the shuttle orbiter must initially park near the target object, preferrably in the same orbit. Then the retrieval package is deployed and transferred to the object such that rendezvous is along its spin axis. It is very desirable and possibly essential to have an optimized transfer trajectory, either to minimize time or fuel (impulse) for the maneuver. The optimization technique used must handle a special terminal state constraint, spin axis alignment. This represents a difficult problem because it leads to a three-dimensional trajectory (out-of-the-plane). The transfer represents a solution to a nonlinear boundary value problem with a terminal constraint on the approach direction.

II. Optimization Methods

An investigation of various optimization techniques has shown that a conjugate-gradient method should yield valid results with a reasonable amount of computational time. The conjugate-gradient approach attempts to combine the advantages of both first and second order gradient methods while eliminating some disadvantages. As the number of iterations increases convergence becomes rapid near the optimum solution. In addition, a poor initial guess will yield satisfactory solutions, whereas the first-order method would not.[1]

In a first-order gradient technique the direction of movement is made from a nominal point along the direction of steepest ascent. Most steepest ascent methods tend to give an oscillating approach to the local optimum. A conjugate-gradient method utilizes gradients in fixing the direction of movement, but does not necessarily move in the direction of steepest ascent. In this method searches are performed in a certain set of directions (i.e., conjugate directions) chosen so that the optimum of a quadratic function is found in a finite number of iterations. Quadratic behavior is observed near the optimum in all functions which are expandable in a Taylor series. However, in the general search problem the coefficient matrix of the quadratic term in the objective function is not known and it is not possible to compute conjugate directions in advance.

Various proposals have been made to generate a set of these directions. Fletcher and Powell[2] have modified a method proposed by Davidon[3] to generate a set of conjugate directions using the gradient, and Fletcher and Reeves[4] have applied a technique suggested by Hestenes and Stiefel[5] in connection with the solution of linear equations to find a set of conjugate directions. Lasdon, Mitter, and Warren[6] have extended the Fletcher-Reeves conjugate gradient method to function space problems.

The basic problem associated with these methods is the generation of a set of conjugate directions when the form of the quadratic is unknown. It is possible, however, to generate sets of conjugate directions based on a knowledge of the gradients. The method of Fletcher and Reeves uses this idea and appears to be efficient in search and is easily programmed for the digital computer. The Fletcher and Reeves method selects the

direction of search at a given point in accordance with

$$S_{i+1} = -g_{i+1} + \beta_i S_i$$

where g = gradient

$$S = -g$$

$$\beta_i = \frac{\|g_{i+1}\|^2}{\|g_i\|^2} .$$

This method is, therefore, guaranteed to locate the optimum of any quadratic function in at most n stages since this equation generates conjugate directions. For functions which are not quadratic, convergence cannot be guaranteed in n steps. Therefore, a test for convergence is needed. The directions of movement are related to some quadratic approximation, and depending on the type of objective function, convergence to the vicinity of the minimum may be fast or slow. However, once near the optimum, the method converges rapidly, because most functions tend to behave quadratically in this region.

III. Conjugate - Gradient Algorithm

1. Guess control variable u_i; m-vector
2. Solve $\dot{x} = f(x,u,t)$ and $x(t_o)$ = constant forwards; x = state variable, n-vector
3. Solve

$$\dot{\lambda}_k(i) = -\sum_{j=1}^{m} \lambda_j(i) \frac{\partial f_j(i)}{\partial x_k(i)}$$

and

$$\lambda_k(t_f) = \left.\frac{\partial \phi}{\partial x_k(i)}\right|_{t=t_f} , \quad k = 1, \ldots, n$$

backwards

4. Compute $g(u_i) = \frac{\partial H}{\partial u}$

when $H_i = \sum_{k=1}^{m} \lambda_k(i) f_k(i)$

5. $S_o = -g_o$ for i = o

6. Choose $\alpha = \alpha_i$ to minimize $J(u_i + \alpha_i S_i)$

7. $u_{i+1} = u_i + \alpha_i S_i$

8. Go to 2) and 3) with 7)

9. $g_{i+1} = g(u_{i+1})$

10. As $g_{i+1} \simeq 0$

    yes ⟶ stop

    no ⟶ cotinue

11. $\beta_i = \frac{\|g_{i+1}\|^2}{\|g_i\|^2}$

12. $S_{i+1} = -g_{i+1} + \beta_i S_i$

13. Loop to 6)

IV. References for Appendix B

1. Bryson, A. E. and Ho, Y. C., Applied Optimal Control, Gin and Co., Waltham, Mass., 1969.

2. Fletcher, R. and Powell, M. J. D., "A Rapidly Convergent Descent Method for Minimization," British Computer Journal, June 1963, pp. 163-168.

3. Davidon, W. C., "Variable Metric Method for Minimization," A. E. C. R and D Rept., ANL-5990 (Rev.) 1959.

4. Fletcher, R and Reeves, C. M., "Function Minimization by Conjugate Gradients," British Computer Journal, July 1964, pp. 149-154.

5. Hestenes, M. R. and Stiefel, E., "Method of Conjugate Gradients for Solving Linear Systems," Rept. 1654, National Bureau of Standards, 1952.

6. Lasdon, L. S., Mitter, S. K. and Warren, A. D., "The Conjugate Gradient Method for Optimal Control Problems," IEEE Transactions on Automatic Control, Vol. AC-12, No. 2, April 1967, pp. 132-138.

APPENDIX C

Deployment Attitude Dynamics and Control

(R. J. Cenker)

I. Introduction

It has been established that a satellite initially rotating about its minor axis (axis of minimum moment of inertia) will experience a transfer of spin axis due to energy dissipation. The final state is one in which stable spin about the major axis (axis of maximum moment of inertia) is established. However, an ambiguity in pointing direction occurs. The spin vector has two possible orientations with respect to the body axes, 180° away from each other. Elimination of this ambiguity through active control is sometimes essential. Application of the AMAPS technique is a particular example of interest here. The situation with ATS-V is another case where the ambiguity arose to result in wrong spin. Control of this ambiguity is the topic of interest here.

II. Summary of Past Work

Effects of energy dissipation on satellite dynamics have been experienced in actual flights[1] and discussed in several analytical treatments[2,3,4,5]. These efforts have, in general, dealt with discussions of the effect of dissipation on the precession rates and the total time required for a satellite to go from one spin state to another. References 2 and 3 describe attitude drift for a symmetrical body and for "n" symmetrical bodies, respectively. Reference 4 discusses the motion of a non-symmetric body in body fixed and inertial coordinates, while Reference 5 illustrates several

methods of modeling the energy dissipation process and describes effects on non-symmetric bodies.

Control of this attitude drift is discussed in References 6,7, and 8. Axisymmetric spacecraft control is proposed in Reference 6, in which a satellite can be maintained in a configuration other than spinning about the axis of maximum inertia. This is done by addition of energy into the system to compensate for energy dissipation. Reference 7 touches briefly on non-symmetric satellite precession control with controlled energy dissipation, and presents numerical examples for symmetric satellites. Control of a non-symmetric satellite is covered in Reference 8, but only for small perturbation angles, i.e., active energy dissipation is used to return the satellite to the desired stable position when it has been perturbed. Thus, none of the control systems proposed to date considers the question of whether the spin vector will align itself with the positive or negative axis of maximum inertia when the spin axis is originally offset by a large amount.

III. Analysis

Constant energy motion of a non-symmetric, rigid body, in a torque free environment is geometrically described by Poinsot's motion. This is the motion of an ellipsoid (having axes which are proportional to the moments of inertia of the body) that rolls without slipping on an "invariable plane" while its center is a fixed distance from the plane (see Reference 5, Appendix C). This distance is given by $\frac{\sqrt{2T}}{H}$ when T is the rotational kinetic energy and H is the angular momentum. The allowable paths for this motion

in the body fixed coordinate frames are closed paths called polhodes, each polhode having a fixed discrete energy level.

A logicial extension of this motion for dissipative bodies is a change in the distance from the center of the ellipsoid to the invariable plane, thus a continuous change in polhode curves. Figures 2,3, and 4 illustrate the above concepts,[5] along with a geometric interpretation of the critical point in the tumbling motion, i.e., whether $\tilde{\omega}$ has a positive or negative z component when the energy reaches $H^2/2I_2$ determines the final spin orientation.

Since the nutation angle θ (position of the z axis with respect to the final rotation vector, and therefore the angular momentum vector) is the parameter of concern, equations giving θ as a function of time and/or rotational energy are desirable. Although the equations of motion for a non-symmetric body are elliptical in nature and, therefore, not readily reduced to an analytical solution, limits on the nutation angle can be developed as straightforward functions of the energy state. Consider first the case with the rotational energy below the separatrix energy ($T < H^2/2I_2$). Using the symbols of Reference 5 the following relationships are developed

$$\sin^2\theta_u = \frac{I_2\left(2I_3T - H^2\right)}{H^2\left(I_3 - I_2\right)}$$

$$\sin^2\theta_\ell = \frac{I_1\left(2I_3T - H^2\right)}{H^2\left(I_3 - I_1\right)}$$

where

θ_u = upper limit on nutation angle

θ_ℓ = lower limit on nutation angle

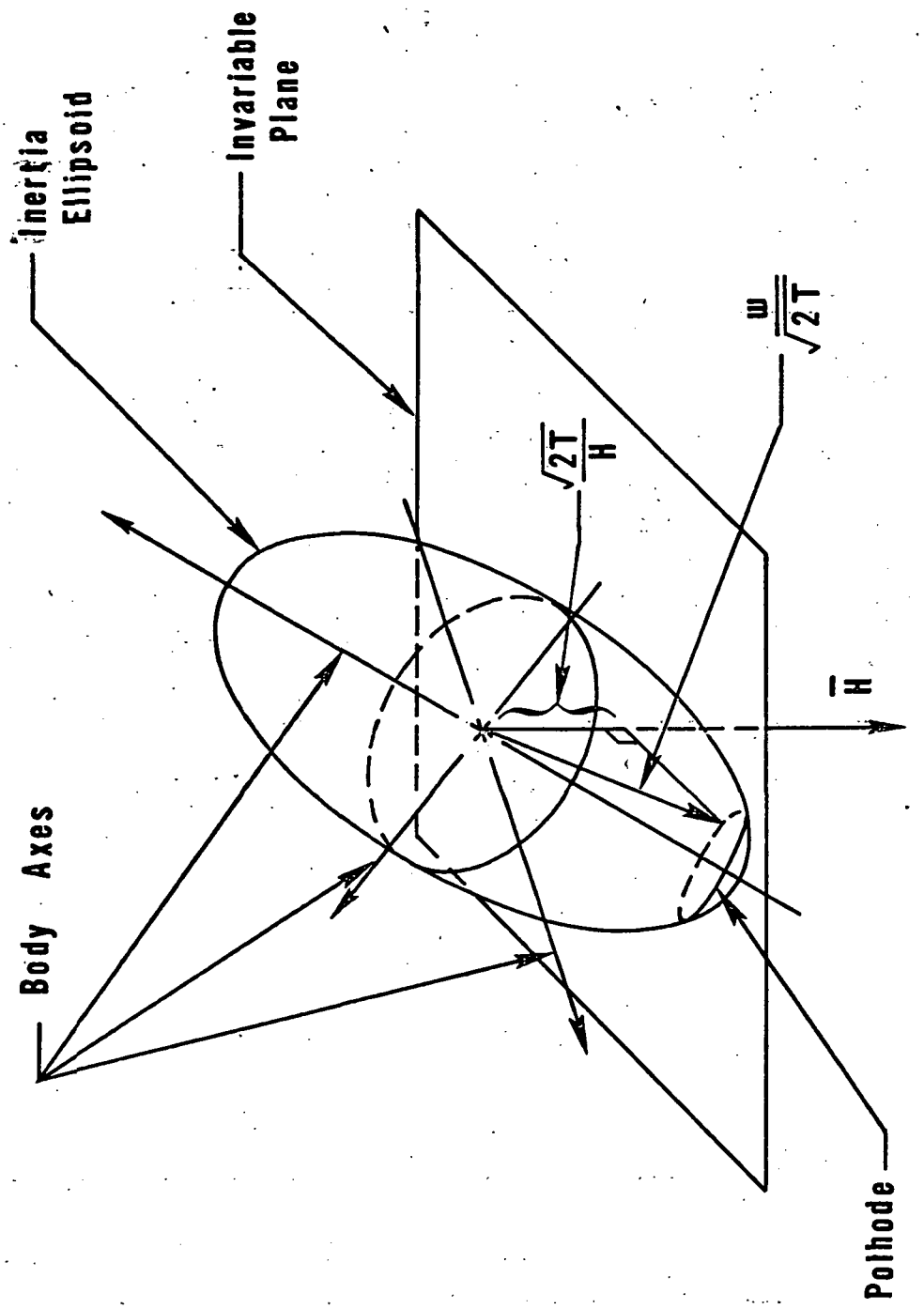

Figure 2. Rigid Body Poinsot Motion

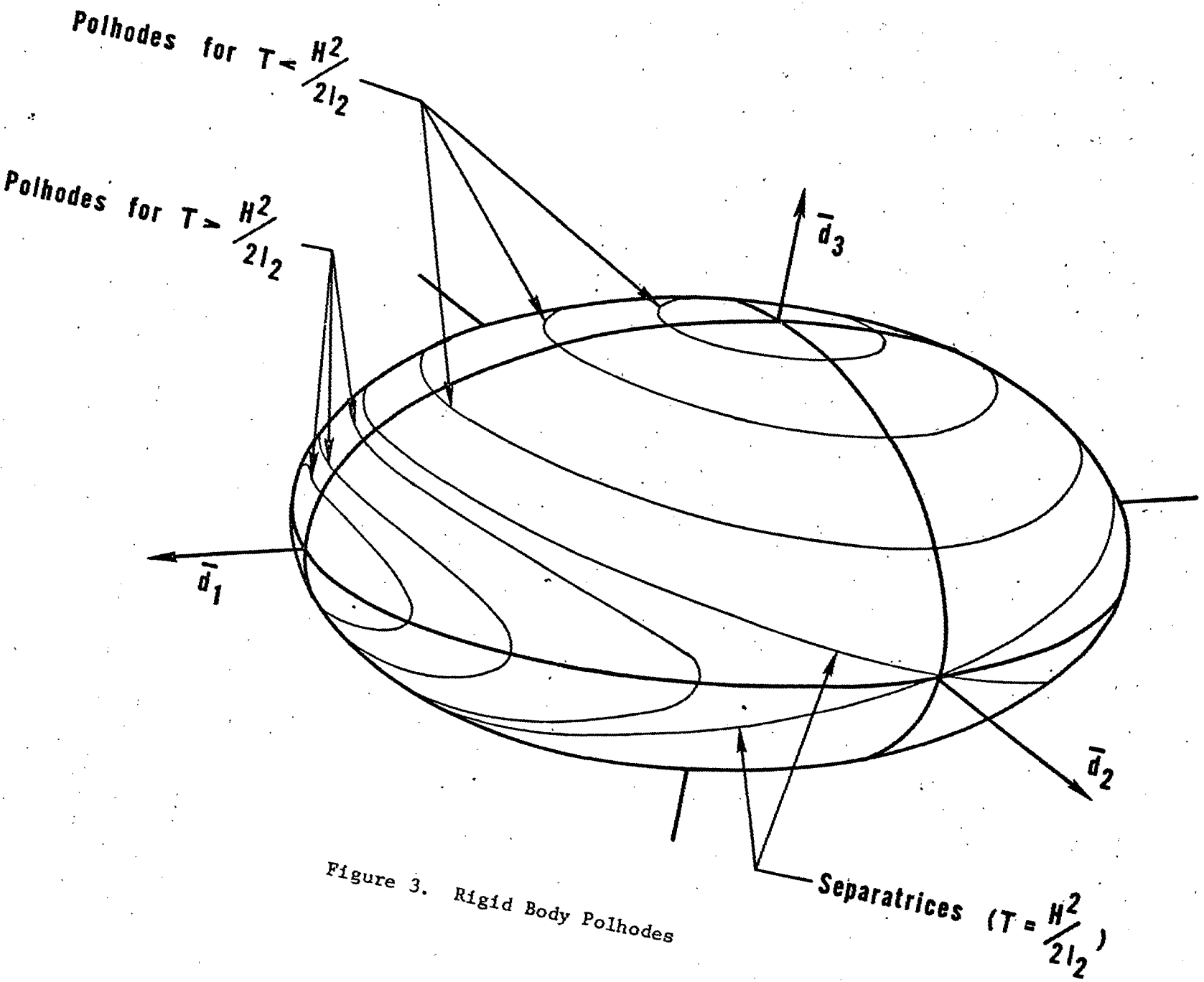

Figure 3. Rigid Body Polhodes

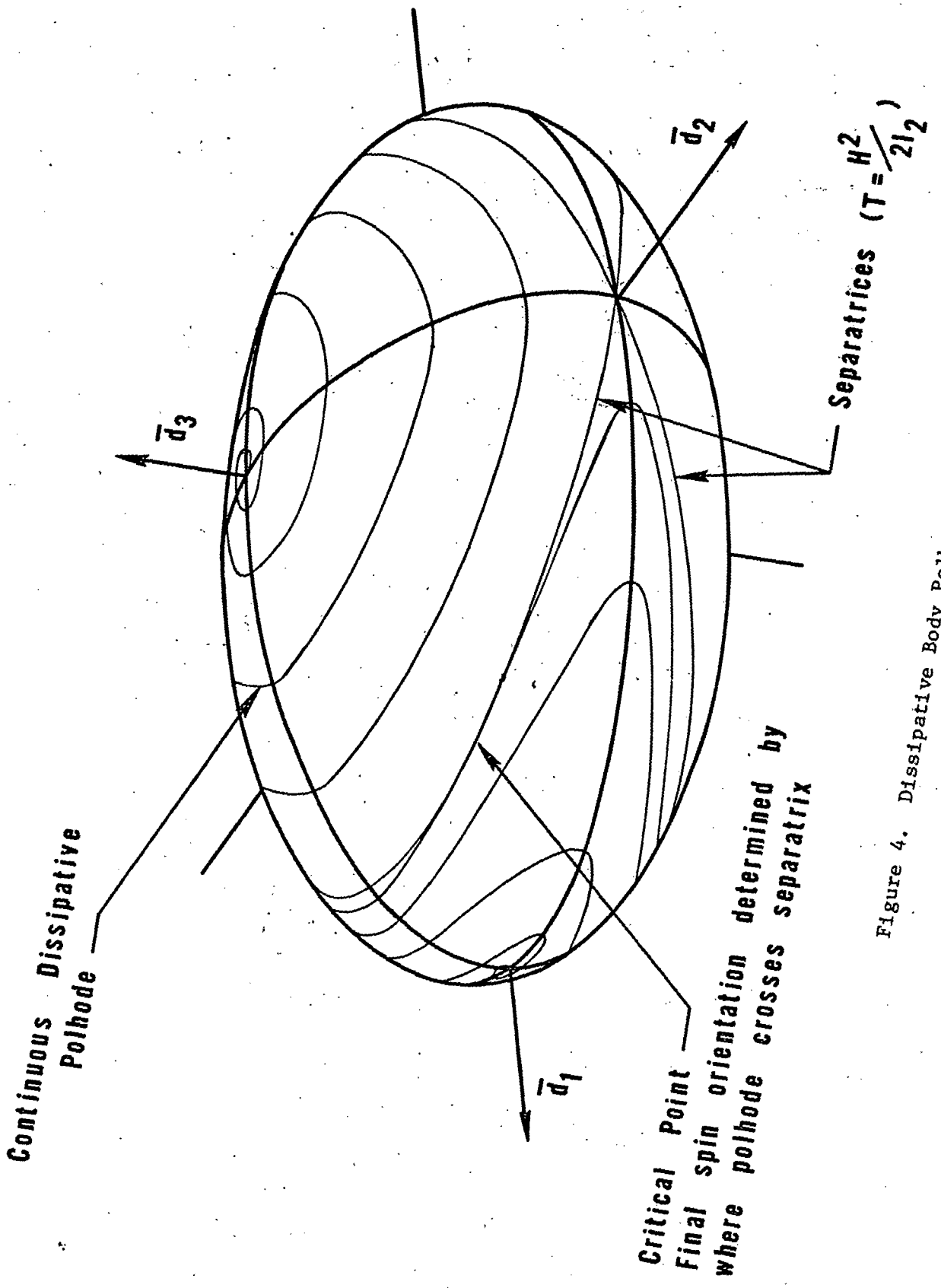

Figure 4. Dissipative Body Polhode

With the energy above the separatrix energy ($T > H^2/2I_2$) the following parallel development can be made. Figure 5 shows the inertia ellipsoid with the z axis in one of its extreme positions. As both extreme positions are similar in nature ($\omega_2 = 0$ and y axis out of the plane of the paper) the upper and lower limits are $90° \pm \theta_{ex}$, respectively.

$$\sin^2\theta_{ex} = \frac{I_3^2\omega_3^2}{H^2} = \frac{I_3}{H^2}\left(2T - I_1\omega_1^2\right)$$

$$= \frac{I_3}{I_1 H^2}\left(2I_1T - H^2 + I_3\omega_3^2\right)$$

The above relations take into account the fact that at this point in the motion

$$\left.\begin{aligned} 2T &= I_1\omega_1^2 + I_3\omega_3^2 \\ H^2 &= I_1^2\omega_1^2 + I_3^2\omega_3^2 \end{aligned}\right\} \quad \omega_2 = 0$$

Further manipulation yields

$$\sin^2\theta_{ex} = \frac{I_3\left(2I_1T - H^2\right)}{H^2\left(I_1 - I_3\right)} + \frac{I_3^2}{I_1H^2\left(I_1 - I_3\right)}\left\{I_3\omega_3^2\left(I_1 - I_3\right) - \left(2I_1T - H^2\right)\right\}$$

Bearing in mind the particular energy and momentum conditions at this point, the final term in brackets equals zero; therefore,

$$\sin^2\theta_{ex} = \frac{2I_1I_3}{H_2\left(I_1 - I_3\right)}T - \frac{I_3}{I_1 - I_3}$$

To provide as general an interpretation as possible, introduce the following terms:

$$I_{13} = \frac{I_1}{I_3}$$

$$I_{12} = \frac{I_1}{I_2}$$

$$T_* = \frac{T}{T_{MAX}}$$

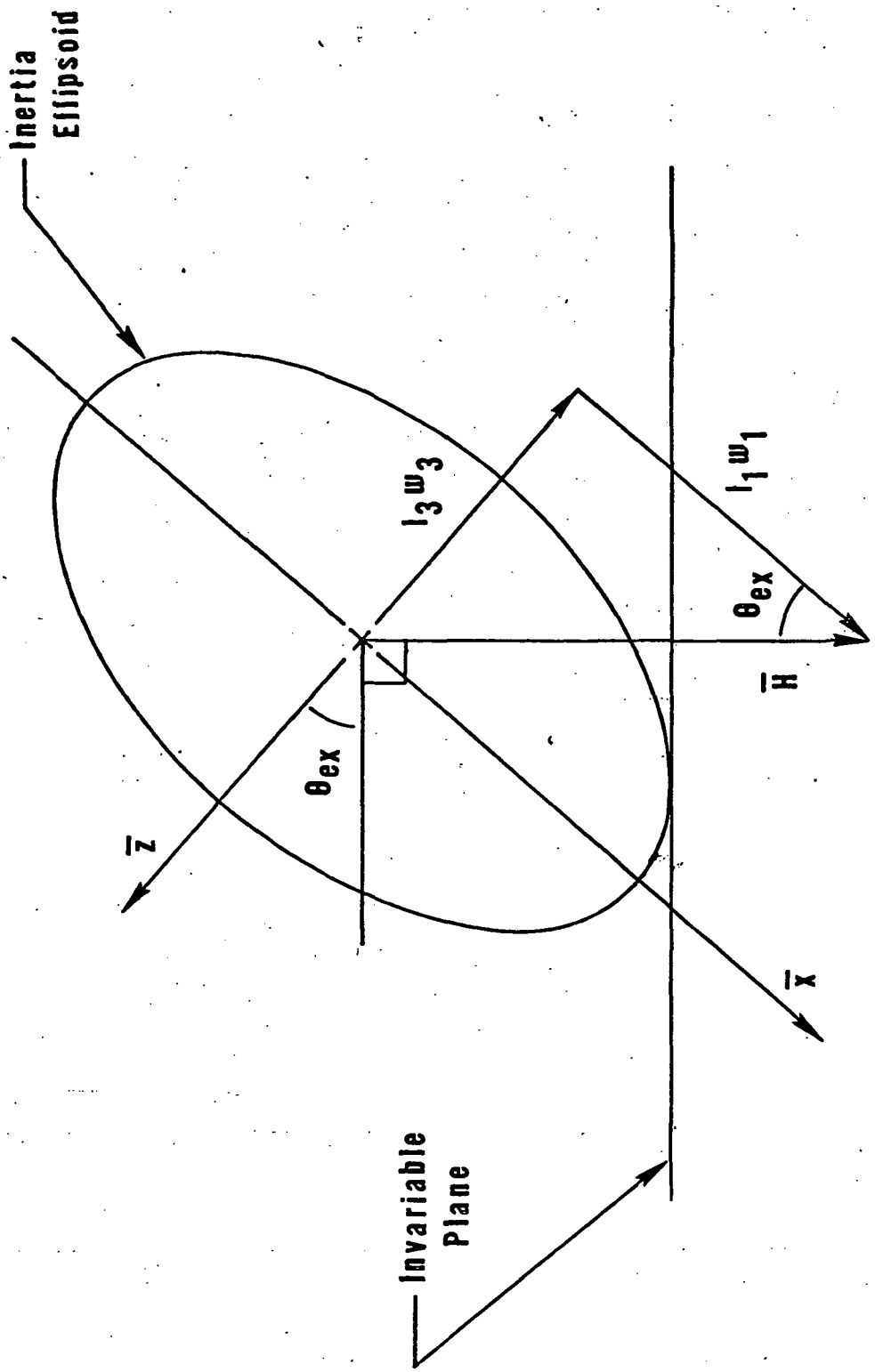

Figure 5. Extreme Position of z Axis

where T_{max} is the maximum possible energy state for a given angular momentum. Thus, $T_{max} = H^2/2I_1$. Making the above substitutions, the bounds on the nutation angle reduce to the following forms:

a. Motion physically below the separatrix ($T > H^2/2I_2$)

$$\theta_{u_b} = 90° + \arcsin\sqrt{\frac{1-T_*}{1-I_{13}}}$$

$$\theta_{l_b} = 90° - \arcsin\sqrt{\frac{1-T_*}{1-I_{13}}}$$

b. Motion physically above the separatrix ($T < H^2/2I_2$)

$$\theta_{u_a} = \arcsin\sqrt{\frac{T_*-I_{13}}{I_{12}-I_{13}}}$$

$$\theta_{l_a} = \arcsin\sqrt{\frac{T_*-I_{13}}{1-I_{13}}}$$

At this stage, two relationships are to be noted:

1) The intermediate moment of inertia (contained in the term I_{12}) has no effect on the nutation angle range below the separatrix, and no effect on the lower limit of θ above the separatrix.

2) At the separatrix

$$T = \frac{H^2}{2I_2}$$

$$\therefore T_* = \frac{I_1}{I_2} = I_{12}$$

Therefore, the upper limit on θ is 90°. For a specific body having a minimum to maximum inertia ratio of one half ($I_{13} = 0.5$) the range of T_* is given by $0.5 \leq T_* \leq 1.0$. Figure 6 shows a plot of the bounds on θ vs T_*, assuming that $I_{12} = I_{13}$. Therefore, the first pair of equations holds for the entire range of T_*. Figure 7 shows the bounds on θ for a body having the same I_{13}, but with an intermediate ratio, $I_{12} = 0.8$. This can be seen as the critical point in the motion, as the bounds on θ divide into two regions:

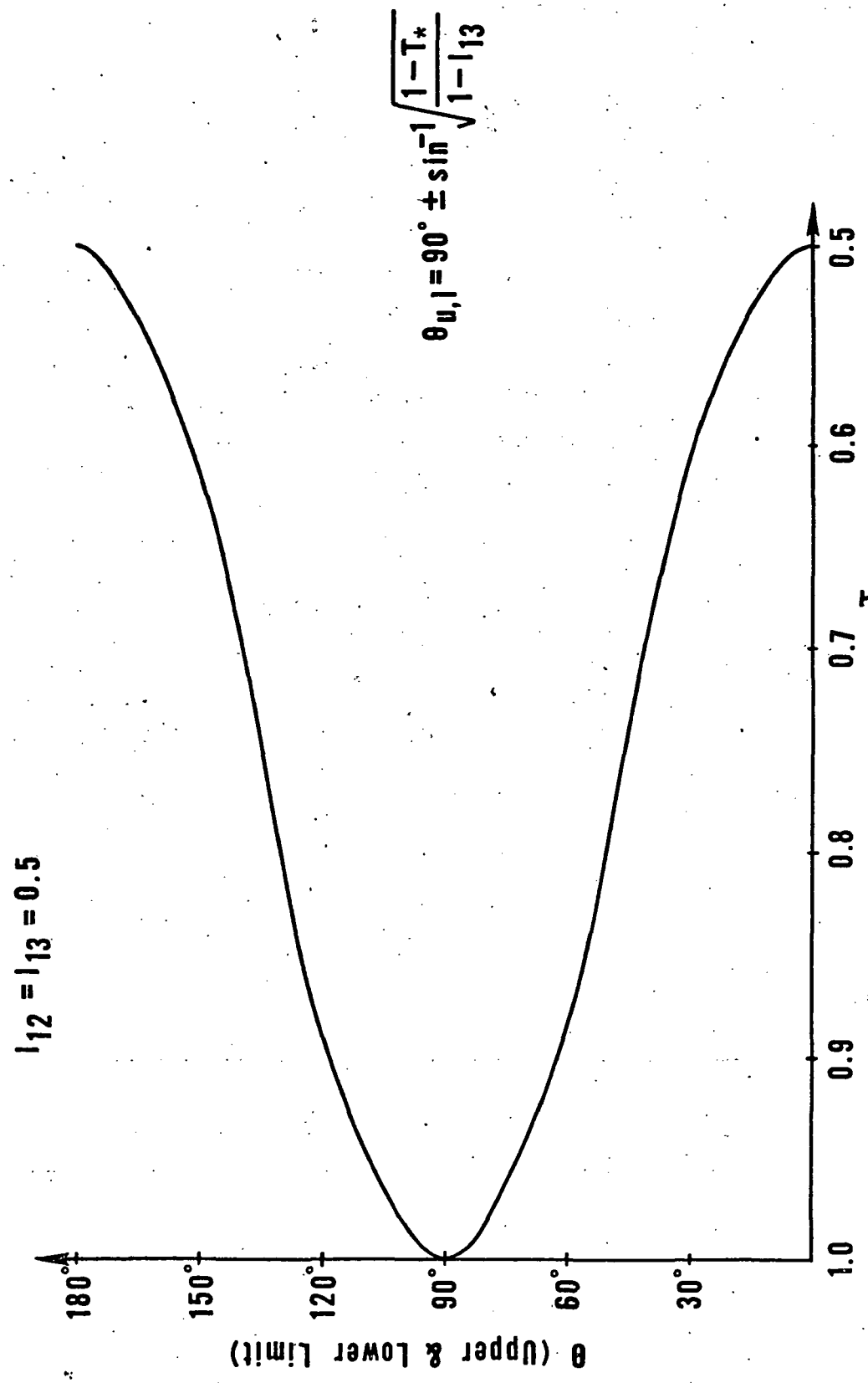

Figure 6. Bounds on θ for Symmetric Dissipative Body

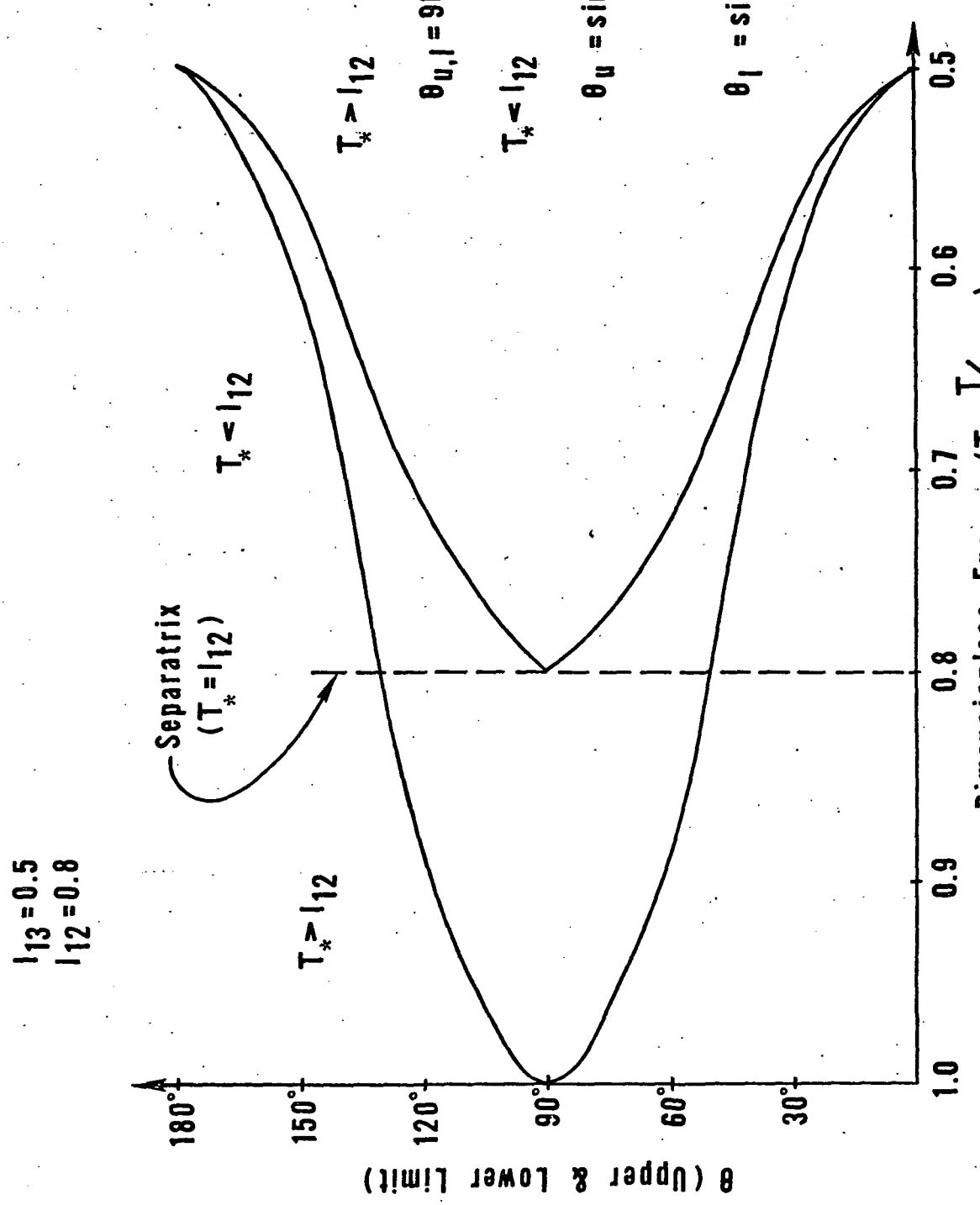

Figure 7. Bounds on θ for Non-Symmetric Dissipative Body

one ending in a final nutation angle of zero ($\tilde{z}$, $\tilde{\omega}$, $\tilde{h}$ pointing in the same direction), the other ending in a final θ of 180° ($\tilde{z}$ pointing in the opposite direction as $\tilde{\omega}$ and $\tilde{h}$).

Noting the continuity of the minimum values for θ at the transition point, the following relations can be written:

$$\theta_{l_a} = 90° - \arcsin\sqrt{\frac{1-T_*}{1-I_{13}}}$$

$$= \arccos\sqrt{\frac{1-T_*}{1-I_{13}}}$$

$$\theta_{l_a} = \arcsin\sqrt{\frac{T_*-I_{13}}{1-I_{13}}}$$

$$\cos^2\theta_{l_b} = \frac{1-T_*}{1-I_{13}} \quad , \quad \sin^2\theta_{l_a} = \frac{T_*-I_{13}}{1-I_{13}}$$

$$\cos^2\theta_{l_b} + \sin^2\theta_{l_a} = \frac{1-I_{13}}{1-I_{13}} = 1$$

$$\therefore \quad \theta_{l_b} = \theta_{l_a}$$

This coincides with the earlier observation that I_{12} did not affect the bounds θ_{l_b}, θ_{μ_b}, and θ_{l_a}, as the value for I_{12} has no effect on these portions of the curve.

From the above description of tumbling motion it is apparent that the critical point in the motion is where the energy satisfies

$$T = H^2/2I_2$$

At this point either the nutation angle or the z component of $\tilde{\omega}$ identifies which direction the final spin vector will assume. Final control over this direction will be attempted by assuming some realistic energy dissipation rate[9] and either changing the moment of inertia by moving some mass within the spacecraft, or altering the energy state by starting an electric motor within the satellite. At this point, any changes in the moments of inertia are expected to use symmetrical motions of masses to avoid shifting of the center of mass of the satellites, simplifying the resulting equations of motion. Present plans also call for lining up any control motor with the z axis, as this component of the rotation appears the most critical.

IV. Conclusions

Results to this point yield a critical state at the point where $T = H^2/2I_2$. At this point, either the nutation angle or the z component of the rotation vector can be used to predict the final spin orientation, according to the following criteria.

$\left.\begin{array}{l}\theta > 90^\circ \\ \omega_3 < 0\end{array}\right\}$ FINAL $\tilde{\omega}$ ALONG $-\tilde{z}$

$\left.\begin{array}{l}\theta < 90^\circ \\ \omega_3 > 0\end{array}\right\}$ FINAL $\tilde{\omega}$ ALONG $\tilde{z}$

Prior to this point ($T = H^2/2I_2$) the z axis oscillates about 90° from the angular momentum vector. After passing this point, it oscillates through a steadily decreasing range to either 180° or 0° from $\tilde{h}$. Control

over this final orientation will be sought rising either available hardware on the spacecraft (extendable booms, electric motors) or equipment designed especially for control purposes. A computer simulation will be developed to demonstrate the feasibility of the scheme, and areas of potential improvement or difficulty will be identified.

V. References for Appendix C

1. ... "Final Report on a Study of Automated Rendezvous and Docking for ATS-V Despin," Space Division, North American Rockwell, Contract NASW-2136, February 1971.

2. Thomson, W. T. and Reiter, G. S., "Attitude Drift of Space Vehicles," Journal of the Astro. Sciences, No. 7, 1960, pp. 29-34.

3. Vigneron, F. R., "Motion of Freely Spinning Gyrostat Satellites with Energy Dissipation," Astronautica Acta, Vol. 16, 1971, pp. 373-380.

4. Kuebler, M. E., "Gyroscopic Motion of an Unsymmetrical Satellite under no External Forces," NASA Tech. Note D-596, July 1960.

5. Likins, P. W., "Effects of Energy Dissipation on the Free Body Motions of Spacecraft," J.P.L. Tech. Rep. 32-860, July 1966.

6. Hopper, F. W., "Active Precession Control for Spin Stabilized Space Vehicles," AIAA Paper #71-952, presented at AIAA Guid., Control and Flight Mechanics Conference, August 16-18, 1971.

7. Kane, T. P. and Scher, M. P., "A Method of Active Attitude Control Based on Energy Considerations," Journal of Spacecraft and Rockets, Vol. 6, No. 5, 1969, pp. 633-636.

8. Alper, J. R., "Analysis of Pendulum Damper for Satellite Wobble Damping," Journal of Spacecraft and Rockets, Vol. 2, No. 1, 1964, pp. 50-54.

9. Kaplan, M. H. and Beck, N. M., "Attitude Dynamics and Control of Apogee Motor Assembly with Paired Satellites," Journal of Spacecraft and Rockets, June 1972, pp. 410-415.

APPENDIX D

Automatic Control Systems for the Retrieval Package

(A. A. Nadkarni)

I. Dynamics and Control during Capture with Spin Axis Misalignment

The analysis used to predict disturbed motion of a spinning object due to accidental application of a torque by the ring[1] is extended to a more general case of spin-vector misalignment. Increased divergence of the composite body (target plus ring together) during despin is considered. Associate control systems and limitations and misalignment are being studied in addition to an appropriate damper for stabilizing the dynamics.

At least a small alignment error can always be expected during the retrieval sequence. The general situation considered is illustrated in Figure 8. It is assumed that $\bar{\omega}_s \simeq \bar{\omega}_r$, i.e., the two spin vectors are approximately synchronized before capture. To calculate the resultant angular momentum of the total system after capture use[2]

$$H = \overline{H}_o + \overline{H}_1 + \overline{r}_p \times m_o \dot{\overline{r}}_p + \overline{r}_1 \times m_1 \dot{\overline{r}}_1 \qquad (1)$$

where $\bar{H}_o$ and $\bar{H}_1$ represent the angular momenta of the reference body and satellite about their respective centers of mass.

Referring to Figure 8, the total angular momentum about the composite center of mass C is

$$\overline{H}_c = \overline{H}_o + \overline{H}_1 + \overline{\rho}_1 \times m_1 \dot{\overline{\rho}}_1 - \overline{\rho}_c \times m \dot{\overline{\rho}}_c \qquad (2)$$

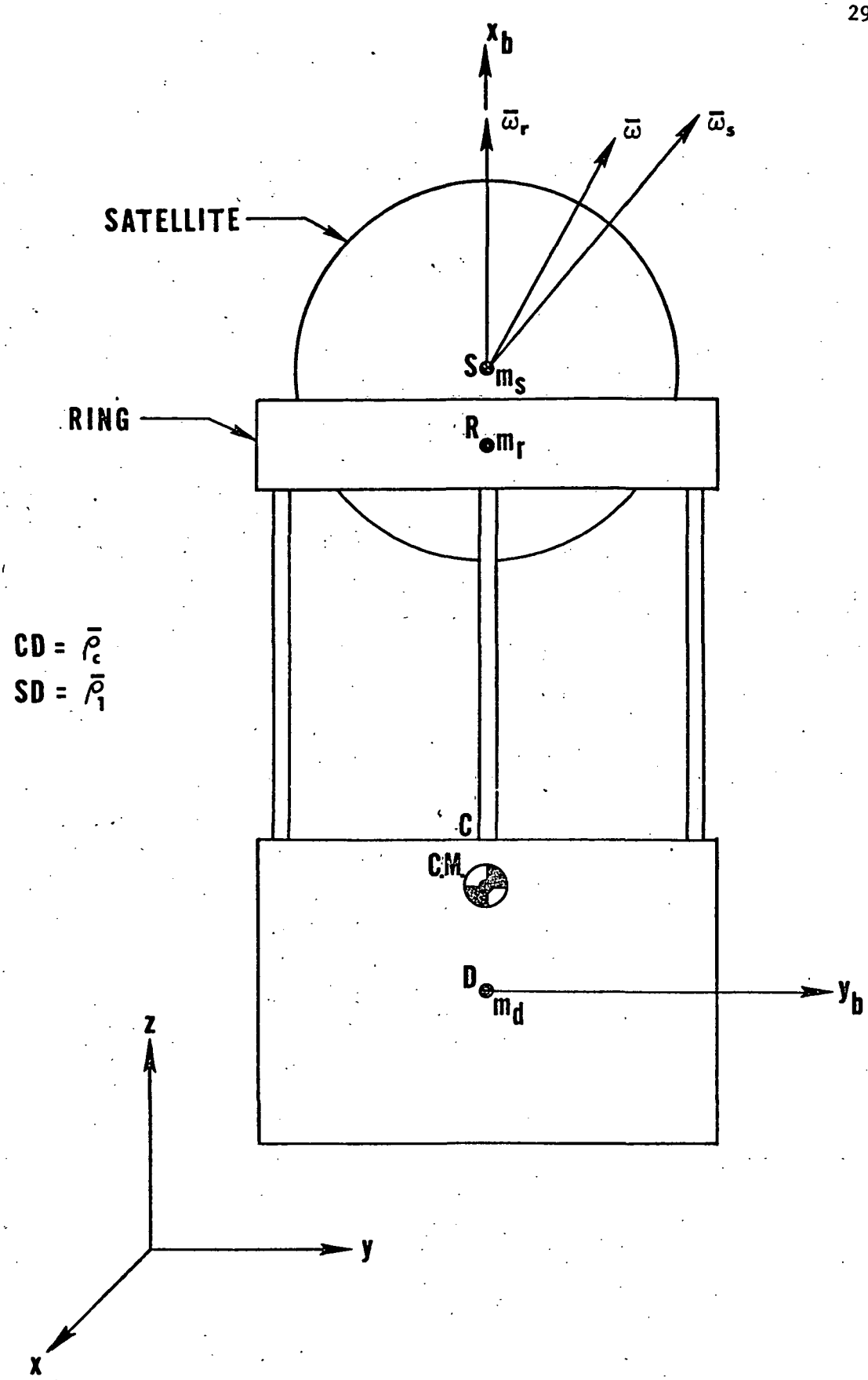

Figure 8. General Misalignment of the Spin Vector

where

$$m = m_0 + m_1 = m_r + m_s$$

Now using

$$\begin{aligned} \dot{\bar{\rho}}_1 &= (\dot{\bar{\rho}}_1)_r + \bar{\omega}_0 \times \bar{\rho}_1 \\ \dot{\bar{\rho}}_c &= (\dot{\bar{\rho}}_c)_r + \bar{\omega}_0 \times \bar{\rho}_c \\ \bar{\omega}_0 &= \bar{\omega}_r \end{aligned} \tag{3}$$

equation (2) may be written as

$$\bar{H}_c = \bar{H}_p' + \bar{H}_p'' - \bar{\rho}_c \times m (\dot{\bar{\rho}}_c)_r - \bar{\rho}_c \times m (\bar{\omega}_0 \times \bar{\rho}_c) \tag{4}$$

where

$$\begin{aligned} \bar{H}_p' &= \bar{H}_0 + \bar{H}_1' + \bar{\rho}_1 \times m_1 (\bar{\omega}_0 \times \bar{\rho}_1) \\ \bar{H}_p'' &= \bar{H}_1'' + \bar{\rho}_1 \times m_1 (\dot{\bar{\rho}}_1)_r \\ \bar{H}_1' &= [I_1] \{\omega_r\} \\ \bar{H}_1'' &= [I_1] \{\Omega_1\} \\ \bar{\omega}_s &= \bar{\omega}_r + \bar{\Omega}_1 \end{aligned}$$

The total angular velocity of the composite body (satellite and despin package with ring) is given by

$$\bar{\omega}^2 = \frac{\bar{H}_c}{\bar{\bar{I}}_s + \bar{\bar{I}}_r + \bar{\bar{I}}_d} = \frac{\bar{H}_c}{\bar{\bar{I}}} \tag{5}$$

Now, using generalized momenta

$$p_\psi = \frac{\partial T}{\partial \dot{\psi}}$$

$$p_\theta = \frac{\partial T}{\partial \dot{\theta}} \tag{6}$$

$$p_\phi = \frac{\partial T}{\partial \dot{\phi}}$$

we obtain Lagrange's equations of motion

$$\frac{dp_\psi}{dt} = M_\psi \tag{7}$$

$$\frac{dp_\theta}{dt} - \frac{\partial T}{\partial \theta} = M_\theta \tag{8}$$

$$\frac{dp_\phi}{dt} - \frac{\partial T}{\partial \phi} = M_\phi \tag{9}$$

For free motion

$$M_\psi = M_\theta = M_\phi = 0 \tag{10}$$

Choosing the direction of $\dot{\psi}$ as being opposite to H_c, we see that

and
$$p_\psi = -H \tag{11}$$

$$p_\theta = 0 . \tag{12}$$

The solutions for $\dot{\psi}$, $\dot{\theta}$, and $\dot{\phi}$ may now be written as[2]

$$\dot{\psi} = -H\left(\frac{\sin^2\phi}{I_{yy}} + \frac{\cos^2\phi}{I_{zz}}\right) \tag{13}$$

$$\dot{\theta} = H\left(\frac{1}{I_{zz}} - \frac{1}{I_{yy}}\right)\cos\theta \sin\phi \cos\phi \tag{14}$$

$$\dot{\phi} = H\left(\frac{1}{I_{xx}} - \frac{\sin^2\phi}{I_{yy}} - \frac{\cos^2\phi}{I_{zz}}\right)\sin\theta \tag{15}$$

where $\bar{H} = \bar{H}_c$. The energy integral gives

$$I_{xx}\omega_x^2 + I_{yy}\omega_y^2 + I_{zz}\omega_z^2 = \kappa \tag{16}$$

or

$$\frac{I_{zz}-I_{yy}}{I_{zz}I_{yy}}\cos^2\theta\cos^2\phi = \frac{-(\kappa I_{yy}-H^2)}{H^2 I_{yy}} + \frac{I_{yy}-I_{xx}}{I_{xx}I_{yy}}\sin^2\theta \tag{17}$$

By substitution of (17) into (14), it is seen that sin θ is a Jacobian elliptic function of a linear function of time. Comparison of the solutions of this type yields the modulus K of the elliptic functions,

$$K^2 = \frac{(I_{zz}-I_{yy})(H^2-I_{xx}\kappa)}{(I_{yy}-I_{xx})(I_{zz}\kappa - H^2)} \tag{18}$$

and

$$\lambda^2 = \frac{(I_{yy}-I_{xx})(I_{zz}\kappa - H^2)}{I_{xx}I_{yy}I_{zz}} \tag{19}$$

Solving for the Eulerian angles θ, ψ, and ϕ in terms of elliptic functions[3] we have,

$$\cos\theta\cos\phi = \frac{(1-2q\cosh 2\gamma+\dots)(\cos\mu t+q^2\cos 3\mu t+\dots)}{(\cosh\gamma+q^2\cosh 3\gamma+\dots)(1-2q\cos 2\mu t+2q^4\cos 4\mu t+\dots)} \tag{20}$$

$$\cos\theta\sin\phi = \frac{(1+2q\cosh 2\gamma+\dots)(\sin\mu t-q^2\sin 3\mu t+\dots)}{(\cosh\gamma+q^2\cosh 3\gamma+\dots)(1-2q\cos 2\mu t+2q^4\cos 4\mu t+\dots)} \tag{21}$$

$$\sin\theta = \frac{(\sinh\gamma-q^2\sinh 3\gamma+\dots)(1+2q\cos 2\mu t+\dots)}{(\cosh\gamma+q^2\cosh 3\gamma+\dots)(1-2q\cos 2\mu t+\dots)} \tag{22}$$

and

$$e^{-2i\psi} = \text{const.}\ \frac{\vartheta_{01}}{\vartheta_{01}}\ \frac{\left(\frac{\lambda t-ia}{2K}\right)}{\left(\frac{\lambda t+ia}{2K}\right)}\cdot e^{\left\{\frac{2iH}{I_{zz}}+\frac{\lambda}{K}\frac{\vartheta_{01}'\left(\frac{ia}{2K}\right)}{\vartheta_{01}\left(\frac{ia}{2K}\right)}\right\}t} \tag{23}$$

The constant of integration may be calculated from the initial conditions. Thus, the motion of the composite body is given in terms of the Eulerian angles as functions of time.

The angular speed of the composite body will be maintained provided the spin rate of the design ring is constant. After capture of the satellite,

the retrieval package control system switches off the despin motor. The ring and satellite are then despun to zero angular velocity before the retrieval package returns to the shuttle. Assuming that the despinning operation takes a finite amount of time, we can assume a linear decay law for the non-constant spin rate,

$$p = \frac{p_0}{(1+at)} \tag{24}$$

From Euler's equations of motion, assuming that the body is approximately mass symmetric about the rotational axis, we may write,[4]

$$M_y + iM_z = I(\dot{q}+i\dot{r}) + ip(I-I_{xx})(q+ir) \tag{25}$$

and

$$\dot{\lambda} = \dot{\theta} + i\dot{\psi} = (q+ir)e^{i\phi} \tag{26}$$

where use has been made of $\cos\theta \simeq 1$ and $\psi \sin\theta \ll p$. Combining equations (25) and (26), yields

$$\ddot{\lambda} + \dot{\lambda}\left(-ip\frac{I_x}{I}\right) = \left(\frac{M_y+iM_z}{I}\right) e^{i\int_0^t p\,dt + \phi_0} \tag{27}$$

Equation (27) governs the pitching and yawing motions, with respect to the space axis, of the rotationally symmetric bodies with non-constant spin rates.

The general form of the solution to (27) is

$$\begin{aligned}\lambda = \theta + i\psi &= e^{i\phi_0}\int_0^t \left[e^{i\int_0^t p\frac{I_x}{I}dt}\right]\left[\int_0^t \left(\frac{M_y+iM_z}{I}\left\{e^{i\int_0^t p\left(1+\frac{I_x}{I}\right)dt}\right\}\right)dt\right. \\ &\left. + \dot{\lambda}_0 e^{-i\phi_0}\right]dt + \lambda_0\end{aligned} \tag{28}$$

Equations for θ and ψ could be obtained by separation of the real and the imaginary parts of equation (28)[4]

II. Despin Ring Speed Control

Once the retrieval package is aligned with the spin axis of a target satellite the despin ring is spun up to the same angular rate as the target. After the speeds are synchronized capture arms extend inward to the satellite. As these arms move inward the inertia characteristics of the ring are changed and its speed will increase. A control system is desired to maintain the speed as constant as possible while the inertia changes. An initial system design with feedback proved to be unstable with the values of the variables chosen as being typical. A compensated system was then design with another feedback loop which greatly increased stability.

The voltage E_f applied to the field is obtained from the output of an amplifier in low-power operation or from a dc generator when greater power is required. In the field circuit, the resistance of the windings is R_f, and the inductance is designated by L_f.

The torque T developed by a motor is proportional to the product of the armature current I_a and the magnetic flux ϕ of the field:

$$T = K_o \phi I_a$$

where K_o is a constant for any motor and depends upon the total number of armature conductors, the number of poles, etc.

A typical curve of flux ϕ versus field current I_f is shown in Figure 9. When the field current I_f becomes great enough to cause the iron to saturate, the flux ϕ no longer increases linearly with the current. Motors used in control systems usually operated over

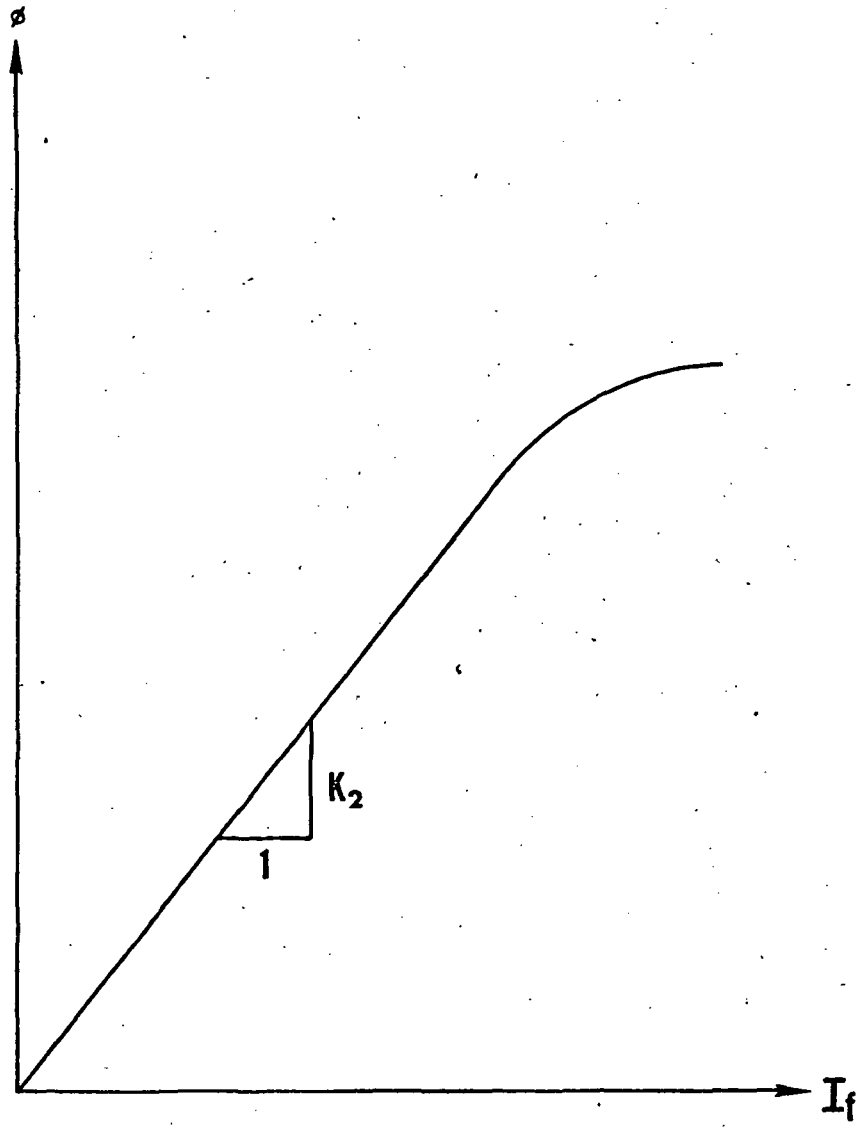

Figure 9. Plot of Flux vs. Field Current

linear portion of this curve, in which case:

$$\phi = K_2 I_f$$

where K_2 is the slope of the linear portion of the curve shown in Figure 9. Therefore, we may write:

$$T = K_0 K_2 I_a I_f = K_m I_a I_f$$

where

$$K_m = K_0 K_2 .$$

If the moment of inertia of the armature is J, the coefficient of viscous friction B_v, and the load torque T_L, then from a summation of torques acting on the armature it follows that

$$T = (B_v D + J D^2) + T_L$$

where

$$D = \frac{d}{dt} .$$

The equation for the field current I_f is obtained from the equivalent field circuit

$$I_f = E_f / (R_f + L_f D) = E_f / R_f (1 + \tau_f D)$$

where $\tau_f = \frac{L_f}{R_f}$ is the time constant of the field circuit.

The circuit equation for the armature is then

$$\begin{aligned} (E_r - K_c \dot{\theta}_c) K_1 &= R_f \left(1 + \frac{L_f}{R_f} D\right) I_f \\ &= I_f R_f + I_f L_f D \\ &= R_f (1 + \tau_f D) I_f \end{aligned}$$

where $E_r = K_r \dot{\theta}_r$ (command input)

and $E_c = K_c \dot{\theta}_c$ voltage signal from tachometer

The transfer function is defined as follows where $C = \frac{I_a}{R_f}$

$$\left\{ (\dot{\theta}_r K_r - \dot{\theta}_c K_c) \left[\frac{K_1 K_m C}{1 + \tau_f D} \right] - T_L \right\} \frac{1}{D(B_r + JD)} = \dot{\theta}_c$$

$$\frac{\dot{\theta}_c}{\dot{\theta}_r} = \frac{K_1 K_r K_m C}{\tau_f J D^3 + (B_r \tau_f + J) D^2 + BD + K_1 K_c K_m C}$$

In Laplace form with all initial conditions equal to zero we have

$$\frac{\dot{\theta}_c(s)}{\dot{\theta}_r(s)} = \frac{K_1 K_r K_m C / \tau_f J}{s^3 + \left(\frac{B_r}{J} + \frac{1}{\tau_f} \right) s^2 + \left(\frac{B_r}{J \tau_f} \right) s + \frac{K_1 K_c K_m C}{\tau_f J}}$$

For the disturbance T_L, the transfer function has the form

$$\frac{\dot{\theta}_c(s)}{T_L(s)} = \frac{-\frac{1}{J} \left(\frac{1}{\tau_f} + s \right)}{s^3 + \left(\frac{B}{J} + \frac{1}{\tau_f} \right) s^2 + \left(\frac{B}{J \tau_f} \right) s + \frac{K_1 K_c K_m C}{J \tau_f}}$$

The characteristic equations of the above transfer functions rendered the system to be marginally stable at best for all values of the varied parameters.

Compensation was added to the system and the resulting block diagram appears as in Figure 10.

The characteristic equation for this sytem with $\tau_f \triangleq \tau_2$ and B_v negligable is:

$$S^4 + \frac{1}{\tau_2} S^3 + H \frac{\tau_1}{\tau_2} S^2 + G \frac{\tau_1}{\tau_2} S + \frac{G}{\tau_2} = 0$$

where

$$H \triangleq \frac{K_1 K_c K_m C}{J}$$

$$G \triangleq \frac{K_1 K_r K_m C}{J}$$

The transfer functions thus become

$$\frac{\dot{\theta}_c(s)}{\dot{\theta}_r(s)} = \frac{G \frac{\tau_1}{\tau_2} \left(\frac{1}{\tau_1} + s \right)}{S^4 + \frac{1}{\tau_2} S^3 + H \frac{\tau_1}{\tau_2} S^2 + G \frac{\tau_1}{\tau_2} S + \frac{G}{\tau_2}}$$

and

$$\frac{\dot{\theta}_c(s)}{T_L(s)} = \frac{-\frac{\tau_1}{J} \left(\frac{1}{\tau_2} + s \right) \left(\frac{1}{\tau_1} + s \right)}{S^4 + \frac{1}{\tau_2} S^3 + H \frac{\tau_1}{\tau_2} S^2 + G \frac{\tau_1}{\tau_2} S + \frac{G}{\tau_2}}$$

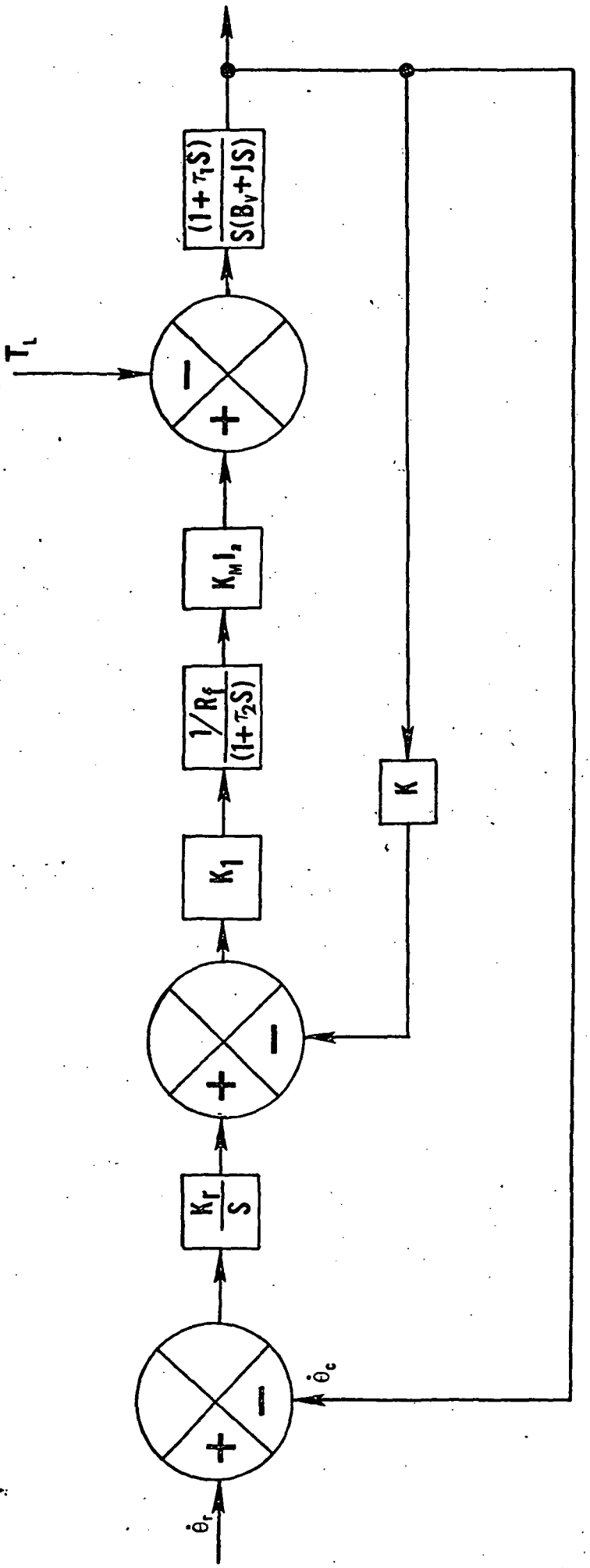

Figure 10. Compensated System

The block diagram for the compensated system appears in Figure 10.

Using the characteristic equation

$$S^4 + \frac{1}{\tau_2} S^3 + H \frac{\tau_1}{\tau_2} S^2 + G \frac{\tau_1}{\tau_2} S + \frac{G}{\tau_2}$$

root-locus diagrams were dran for what was felt to be various typical values of the parameters τ_2 and H.

A good indication of the effect of the ratio τ_1/τ_2 is obtained by constructing the root-locus plot for a small ratio such as $\tau_1/\tau_2 = 4.0$ and for a large ratio such as $\tau_1/\tau_2 = 10.0$.

Tables 1 and 2 show the scheme used for the root-locus plots. The most satisfactory plot is shown in Figure 11.

Here we have a fast τ_2 and a relatively large range on the value of G for stability. The loci were calculated for values of G up to 200 and the system is completely stable. A value of G = 100.0 gives a damping ratio on thb inner loop of $\zeta = 0.95$ with $\beta = 18°$. The natural frequency is $\omega_n = 5.2631$.

The time response of the system appears as

$$\frac{\dot{\theta}_c(t)}{\dot{\theta}_r(t)} = 57.8\, e^{-5t} \sin(1.625t + 151.5°) + 24.4\, e^{-5t} \sin(6.88t + 113.5°)$$

The disturbance time response is

$$\frac{\dot{\theta}_c(t)}{T_L(t)} = \frac{-.437}{J} e^{-5t} \sin(1.625t + 157.66°) + \frac{.201}{J} e^{-5t} \sin(6.88t + 138.1°)$$

$\tau_1/\tau_2 = 4.0$

τ_2 \ H	10	20	40
0.05	U	U	U
0.10	U	S	S
0.50	S	S	S
1.00	U	U	U

U = unstable

S = satisfactory

TABLE 1. Root-Locus Scheme for Small τ_1/τ_2

$\tau_1/\tau_2 = 10.0$

τ_2 \ H	10	20	40
0.05	U	S	S
0.10	S	S	S
0.50	S	S	S
1.00	U	U	U

U = unstable

S = satisfactory

TABLE 2. Root-Locus Scheme for Large τ_1/τ_2

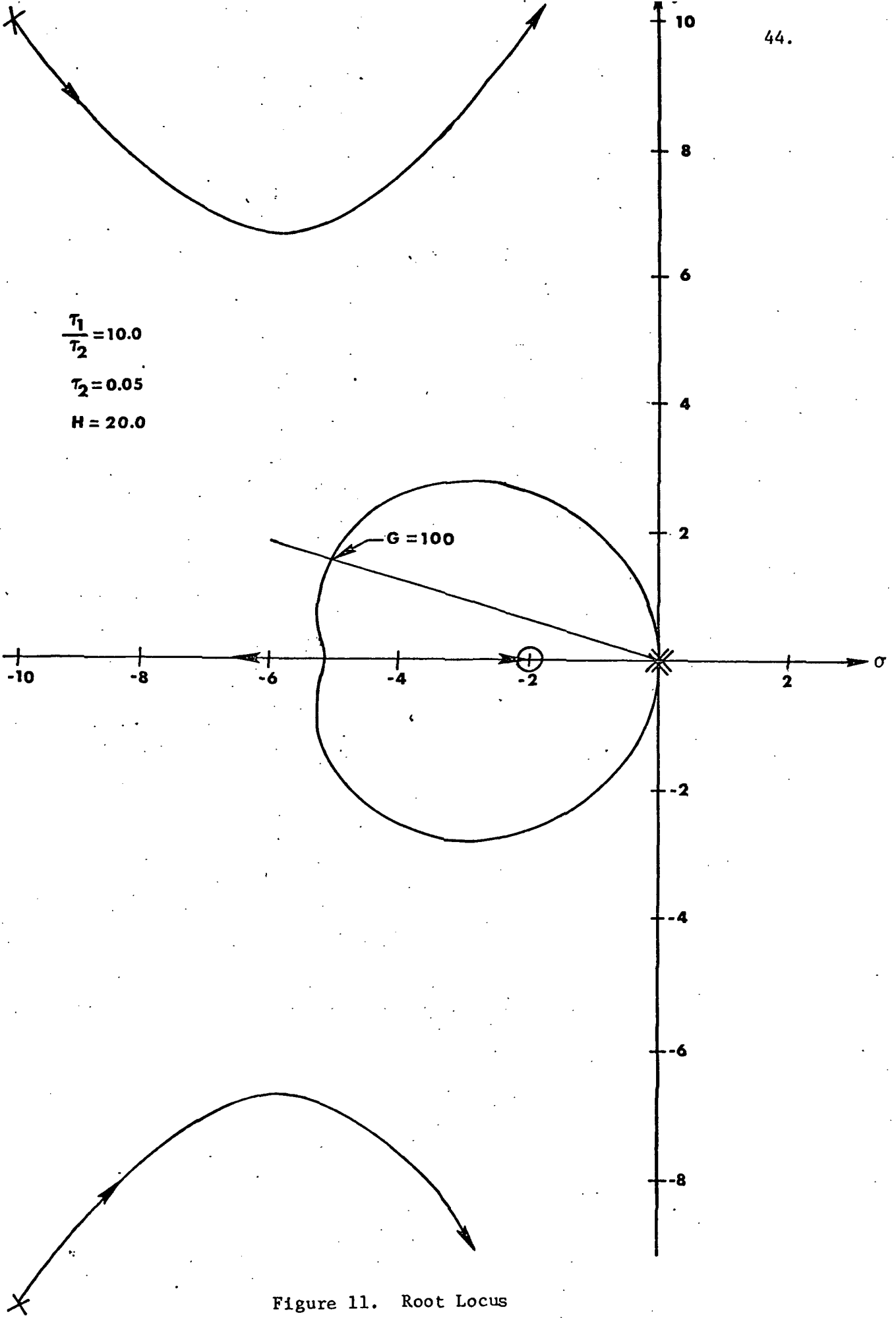

Figure 11. Root Locus

The steady state value for a step reference input are $(\dot{\theta}_c)_{ss} = 1.0$ and for a step disturbance input $(\dot{\theta}_c)_{ss} = -1/(100)J$.

The disturbance torque T_L is due to the changing inertia characteristics of the despin ring. Once the ring is spun up to the speed of the target satellite the capture arms move inward and decrease the inertia of the ring. The angular speed of the ring will increase and be out of sync. with that of the target. The inertia of the ring with the arms fully retracted is 15160.5 lb_m-ft^2 and with the arms fully extended 10360.5 lb_m-ft^2. One might assume the torque T_L to be a linear function of distance. This may be approximated by a ramp function. But at a certain point the arms will stop and the ramp function will level off to a constant value.

In order to resolve this we may regard the input as being the sum of separate functions as is illustrated in Figure 12. The sum of the ramp function which begins at t = 0 and the equal but opposite ramp function which begins at $t = t_o$ is seen to yield the function of Figure 12. The transform of the first ramp function of Figure 12 is x/S^2, and that for the delayed ramp function is $-(x/S^2)e^{-t_o s}$. Thus the transform $T_L(S)$ for the input is

$$T_L(s) = \frac{x}{s^2} - \frac{x}{s^2} e^{-t_o s}$$

Now,

$$\dot{\theta}_c(s) = \frac{-\frac{.5}{J}(s+20)(s+2)x}{(s^2+10s+27.64)(s^2+10s+72.3)s^2}$$

$$\frac{-\frac{.5}{J}(s+20)(s+2)x e^{-t_o s}}{(s^2+10s+27.64)(s^2+10s+72.3)s^2}$$

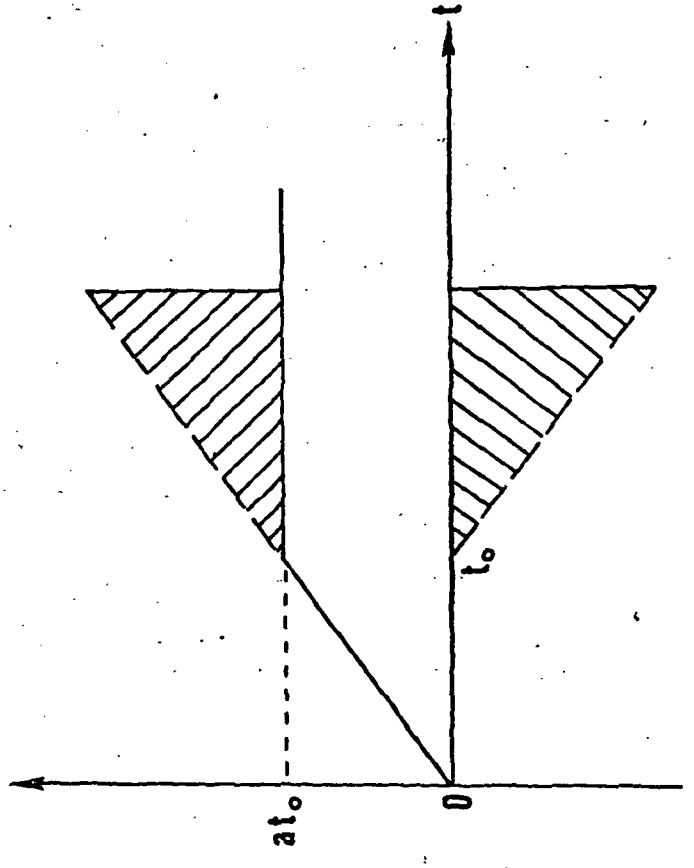

Figure 12. Input Function

Because of the delaying factor $e^{-t_o S}$ the second term on the right-hand side of the above equation should be ignored for $t < t_o$.

III. References for Appendix D

1. Yarber, W. H., "Conceptual Deisgn, Dynamics and Control of a Device for Despinning Orbiting Objects," Astro. Res. Rep. No. 71-2, Penn State University, 1971.

2. Greenwood, D. T., Principles of Dynamics, Prentice-Hall, 1965

3. Whittaker, E. T., A Treatise on the Analytical Dynamics of Particles and Rigid Bodies, Fourth Ed., Dover, New York, 1944.

4. Martz, C. W., "Method for Approximating the Vacuum Motions of Spinning Symmetrical Bodies with Nonconstant Spin Rates," NASA TR R-115, 1961.